Method Development for Spatially Resolved Detection of Adulterated Minced Meat

Ervienatasia Djaw[1], Isik Türkmen[1], Thorsten Tybussek[1], and Tilman Sauerwald[1,2]

[1] Fraunhofer Institute of Process Engineering and Packaging IVV, 85354 Freising, Germany
[2] Saarland University, Department Systems Engineering 66123 Saarbrücken, Germany

Abstract This study explored the possibility of detecting different types of meat in a miniaturized patty by applying a random forest classifier on the spectral dimension followed by neighborhood majority voting on the spatial dimension to improve the random forest prediction. Hyperspectral images of patties made of 100% beef, 100% pork, and 100% horse meat were acquired with a short-wave infrared (SWIR) hyperspectral camera. The pixel-wise meat type prediction by random forest multi-class classifier was accurate to 97.5%. After the majority voting of the neighboring pixels, the prediction accuracy increased to 100%. As next, synthetic hyperspectral images of adulterated patties were generated for validating the model. The prediction accuracy of the model on the synthetic images were bigger than 98%. The findings of the proposed workflow support the development of rapid analysis tools in tandem with machine-learning to detect adulteration in minced meat.

Keywords Hyperspectral imaging, random forest, majority voting, food safety, adulteration, authenticity

1 Introduction

Meat is known for its commercial and nutritional values, yet it is prone to fraudulent and accidental adulteration which violates consumers' safety and protection [1–3]. Besides falsification of meat by other materials than the declared ingredients (e.g. beef/offal), the proportion

of ingredients or the main components (e.g. meat muscles vs fat) may deviate from the stated composition [2, 4, 5]. The DNA-based analysis is the golden standard of authenticating the meat species and their origin, but it's a time-consuming method [3].

Most of the past studies utilized hyperspectral imaging (HSI) in the visible and near-infrared region (VNIR) (450 to 1000 nm) in tandem with chemometrics and artificial intelligence with promising outcomes. Both minced meat and meat cuts can be authenticated via these tools by examining either the whole composition or only the fatty acids profiles [4–9]. However, the spatial information was often left out due to the complexity of the data dimension, and the prediction models were often trained by averaged spectra [4, 6, 8–10]. Ropodi et al. demonstrated the application of multi-spectral imaging in the visible region using 16 spectral features with help of the support vector machine (SVM) giving 93.5% accuracy in detecting horse meat in beef minced meat. The authors also reported that the color-change during storage had a negative influence on the prediction results [6]. Jiang et al. used HSI in the VNIR range coupled with pixel-wise partial least square regression (PLSR) to quantify duck in beef minced meat. The PLSR model was trained by average spectra of patties with different levels of adulteration. Afterwards, the pixel-wise regression was applied in the spatial domain to generate adulteration heat maps [8].

This paper explored the feasibility of detecting different meat species in a patty by using a hyperspectral camera in the short-wave infrared (SWIR) region between 930 to 2500 nm in tandem with a pixel-wise random forest (RF) multi-class classifier, followed by neighborhood majority voting on every pixel across the 2D spatial dimension. The trained RF classifier aimed to classify every pixel into one of three classes as beef, horse or pork, regardless of the meat's freshness level. The neighborhood majority voting was applied subsequently on spatial dimension to improve the pixel-wise classification.

2 Materials and methods

2.1 Meat Sample Preparation and Training Datasets

Minced meat of 100% pork, 100% beef, and 100% horse were purchased from local butchers in Munich, Germany. A patty with ca.10 g of each

meat type was placed on a sterile Petri dish and measured on the purchase day (Day 0) and five days after the purchase day (Day 5). Between Day 0 and Day 5, meat was stored in the fridge at $T = 6 \pm 2°C$. Patties containing different meat types were not used in this study to avoid the uncertainty in the ground truth image pixel labels of those mixtures. Instead, synthetic patties were generated to validate the model. The process of generating synthetic patty is elaborated in section 2.4.

2.2 SWIR hyperspectral imaging system and data acquisition

The SWIR spectra in the region (930 - 2500 nm) were captured using HySpex SWIR 384 SN 3197 (Norsk Elektro Optikk AS, Oslo, Norway) with a 5.45 nm sampling interval which delivers 288 data points per spectrum. The camera was equipped with 1m objective with ca. 84 cm distance between the objective and the sample's surface, resulting in an image resolution of 0.33 mm/px with 32 bit color depth. The samples on the translating stage were exposed to two halogen light sources mounted at a symmetrical angle. The reflection spectra were recorded by the push broom method at an acquisition rate of 33800 µs per spectral line.

2.3 Radiometric Correction and Initial Pre-processing

A radiometric correction was applied to all images using the software HyRad (Norsk Elektro Optikk AS, Oslo, Norway), which adjusted each spectrum based on the reflection of a white reference. The subsequent data preprocessing explained below was performed using the Python 3.9.12 programming language.

Initially the saturated spectral values of a given pixel were replaced by the nearest pixel's unsaturated spectral values or by the averaged spectrum of the surrounding unsaturated pixels [11, 12]. Then the region of interest (ROI) was extracted by removing the irrelevant image sections, such as background, sampling stage, and Petri dish. The ROI extraction process utilized Gaussian blurring filter with a kernel size of (4x4) and 0.5 standard deviations on the grayscale image obtained from the first spectral feature (930 nm) followed by the automatic Otsu thresholding method to create a mask [13,14]. Finally, all spectra within

the mask were extracted and scaled using the 'Standard Scaler' function from scikit-learn python library.

2.4 Random Forest Classification and Dataset

A random forest (RF) multi-class classifier with 100 trees, 'entropy' as the criterion for node-splitting and 20 as the tree's maximum depth, was trained using all spectral features (288 features) in 3 cross-validations. A balanced amount of data across three meat categories were ensured in the training data set. There were 43200 data points from meat measured on Day 0 and 28800 data points from meat measured on Day 5. Not all data points were used for training; the unused data points were set aside to generate synthetic hypercubes in validation stage.

Pixel-Wise Prediction & Majority Class Of The Neighboring Pixels. Every pixel was classified into one of three classes (beef, horse, or pork) by the trained random forest classifier. Consecutively, each prediction result was evaluated spatially by comparing it to the majority class from its surrounding pixels (kernel size 3x3). In case of a class mismatch between the observed pixel and the majority class within the neighbors, the RF prediction probability for all classes of the observed pixel were replaced by the averaged probabilities of its surrounding pixels.

Synthetic Patties For Validation. Synthetic patties (50x50 px) with segmented regions in various shapes, sizes, and grey levels were generated automatically using the function „random_shapes" from the scikit-image python library. Every shape and the background were assigned to a particular class based on its grey level (Figure 5). Sequentially, each pixel was filled with a random spectrum belonging to the assigned class hence generating a hypercube.

3 Results and discussion

As seen in Figure 1, no difference can be observed by the naked eye either between the spectra of different meat types or between fresh and old. Nevertheless, the classification model in this study focused on differentiating the meat types, not the freshness level of the meat. There-

fore, the experiment aimed to generalize 100% beef patty regardless of the mixture of fresh or old beef as a beef patty.

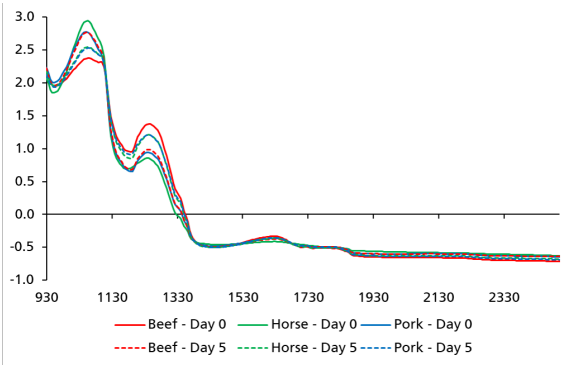

Figure 1: Average spectra of all patties.

Predicted Class	Beef	Horse	Pork
Beef	23111	703	186
Horse	666	23167	167
Pork	116	124	23760
	Beef	Horse	Pork

True Class

Figure 2: Confusion matrix from pixel-wise RF multi-class classifier.

The pixel-wise RF classification gave an accuracy of 97.3%, where 'pork' has the highest precision, recall, and f1-score values (each 99%), followed by 'horse' (each 97%) and 'beef' with 96% recall and 97% of each precision and f1-score. A closer look at the confusion matrix in Figure 2 shows a higher number of falsely predicted 'beef' as 'horse' and vice versa. The mis-classifications from pixel-wise RF classifier were more apparent to occur on single pixels than in a region (Figures 3 and 4, pixel-wise images).

The falsely predicted pixels by pixel-wise RF classifier were corrected by comparing each pixel with its neighbors (majority voting; 3x3 kernel; see 2.4). The significant improvement can be observed in fresh (Figure 3) and five days old patties (Figure 4), comparing the images in

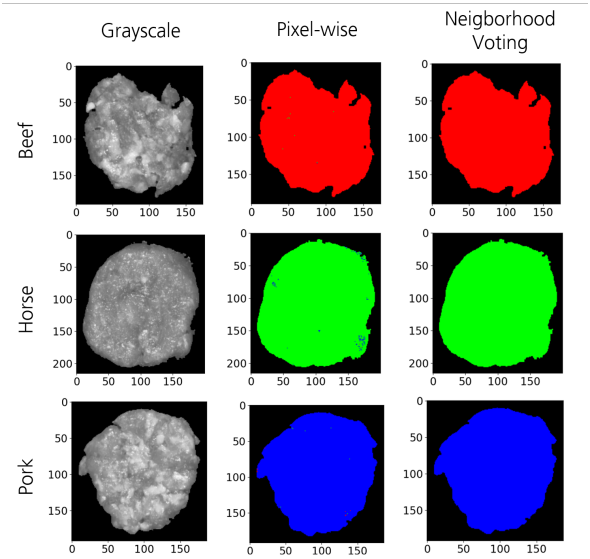

Figure 3: Fresh Meat (Day 0) Classification; Left: grayscale images at 1115 nm; Center: Pixel-wise classification results; Right: Pixel-wise classification results after neighborhood majority voting and probability values correction. Each pixel was colored based on the predicted class: red refers to 'beef', green refers to 'horse', and blue refers to 'pork'.

the middle (pixel-wise) to the images on the right (neighborhood majority voting). The success of the model is remarkably dependent on the correlation between the camera's spatial resolution, the accuracy of pixel-wise prediction, and the kernel size used in neighborhood majority voting.

The spectra at 1115, 930, and 1250 nm respectively appeared to be the most important features observed by RF. The inclusion of these features led to the biggest decrease of a tree's impurity in RF model [15]. These regions refer to the 2nd and 3rd overtone regions of C-H molecular group, except at 930 nm where O-H and C-H are overlap [16]. These findings indicate that a prediction model can be built using only these spectral features, which is to be explored further. For instance, the fat region seems to be in the highest contrast after observing the gray

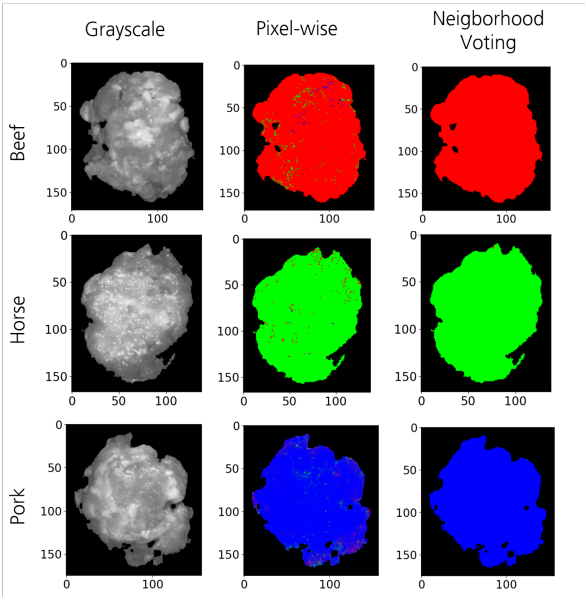

Figure 4: Old Meat (Day 5) Classification; Left: grayscale images at 1115 nm; Center: Pixel-wise classification results; Right: Pixel-wise classification results after neighborhood majority voting and probability values correction.

scale images at 1115 nm (see the pictures on the left in figure 3 and 4). Besides, a study by Lestari et al. demonstrated an improved prediction by using 1D FTIR on the extracted fat from meatballs in detecting rats in beef meatballs [17].

A comparison between patties from day 0 and day 5 shows that false predictions occurred more often on patties from day 5 (Figure 4, middle images) than day 0 (Figure 3 , middle images), as previously stated by Ropodi et al [6]. However, in our case, this could also be due to fewer spectra collected for old patties (day 5) than fresh patties (day 0).

The validation of the complete workflow on synthetic patties showed promising results. The falsely classified pixels were mostly corrected by neighborhood majority voting. The shape of the kernel, which was square altered the shape of regions containing edges, as depicted on the synthetic patty images in figure 5.

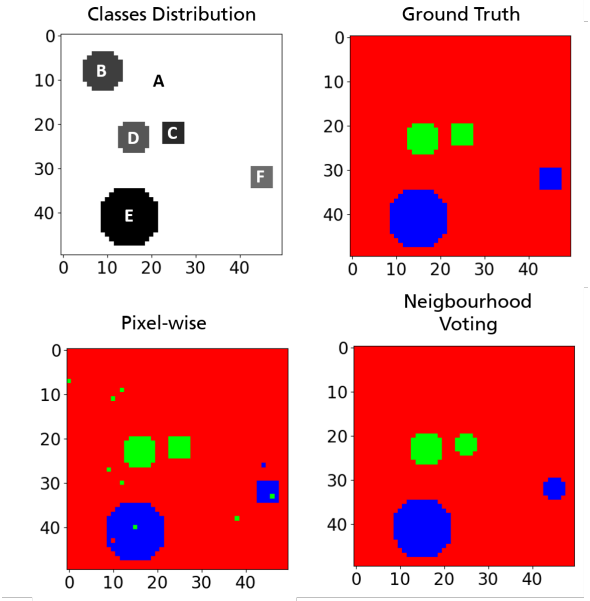

Figure 5: Synthetic Patties with 90.4% beef (A + B or "Red" area), 2.8% horse (C + D or "Green" area), and 6.8% pork (E + F or "Blue" area) of which 2.8% old beef (B), 1.0% old horse (C), and 5.8% old pork (F).

Furthermore, figure 5 also validates the model's generalization, regardless of the freshness level. The old beef spectra (B) were mostly falsely predicted as horse and some of the old pork (E) were predicted as horse or beef.

4 Conclusions and Outlook

Random forest multi-class classification on the spectral dimension followed by neighborhood majority voting in the spatial dimension showed promising results to authenticate minced meat of different types (beef, horse, and pork). The prediction by pixel-wise RF classifier based solely on spectral dimension was accurate to 97.5%. After introducing the majority voting of the neighboring pixels in the spatial

dimension, the prediction accuracy increased to 100%.

The findings of this study can be used to develop rapid analysis tools for minced meat authentication. Furthermore, a prior image processing on the grayscale image to separate high-fat from low-fat regions may also provide an alternative approach, which is to be explored in detail as next.

5 Acknowledgement

This research work was supported by the Leistungszentrum Sichere intelligente Systeme (LZSiS) - Fraunhofer Society of Germany.

References

1. S. Tähkäpää, R. Maijala, H. Korkeala, and M. Nevas, "Patterns of food frauds and adulterations reported in the eu rapid alert system for food and feed and in finland," *Food Control*, vol. 47, pp. 175–184, 2015.
2. K. Robson, M. Dean, S. Brooks, S. Haughey, and C. Elliott, "A 20 year analysis of reported food fraud in the global beef supply chain," *Food Control*, vol. 116, p. 107310, 2020.
3. Y.-C. Li, S.-Y. Liu, F.-B. Meng, D.-Y. Liu, Y. Zhang, W. Wang, and J.-M. Zhang, "Comparative review and the recent progress in detection technologies of meat product adulteration," *Comprehensive Reviews in Food Science and Food Safety*, vol. 19, no. 4, pp. 2256–2296, 2020.
4. M. Kamruzzaman, M. Haque, and M. Ali, "Hyperspectral imaging technique for offal quantification in minced meat," *Journal of the Bangladesh Agricultural University*, vol. 12, no. 1, pp. 189–194, 2014.
5. H. Jiang, F. Cheng, and M. Shi, "Rapid identification and visualization of jowl meat adulteration in pork using hyperspectral imaging," *Foods*, vol. 9, no. 2, p. 154, 2020.
6. A. I. Ropodi, E. Z. Panagou, and G.-J. E. Nychas, "Multispectral imaging (msi): A promising method for the detection of minced beef adulteration with horsemeat," *Food Control*, vol. 73, pp. 57–63, 2017, special issues from the '9th EFFoST International Conference.
7. J. Mendez, L. Mendoza, J. Cruz-Tirado, R. Quevedo, and R. Siche, "Trends in application of nir and hyperspectral imaging for food authentication," *Scientia Agropecuaria*, vol. 10, no. 1, pp. 143–161, 2019.

8. H. Jiang, W. Wang, H. Zhuang, S.-C. Yoon, Y. Yang, and X. Zhao, "Hyperspectral imaging for a rapid detection and visualization of duck meat adulteration in beef," *Food Analytical Methods*, vol. 12, no. 10, pp. 2205–2215, 2019.
9. M. Kamruzzaman, Y. Makino, and S. Oshita, "Hyperspectral imaging in tandem with multivariate analysis and image processing for non-invasive detection and visualization of pork adulteration in minced beef," *Analytical Methods*, vol. 7, no. 18, pp. 7496–7502, 2015.
10. H. Jiang, Y. Yang, and M. Shi, "Chemometrics in tandem with hyperspectral imaging for detecting authentication of raw and cooked mutton rolls," *Foods*, vol. 10, no. 9, p. 2127, 2021.
11. J. Burger and P. Geladi, "Hyperspectral nir image regression part ii: dataset preprocessing diagnostics," *Journal of Chemometrics: A Journal of the Chemometrics Society*, vol. 20, no. 3-4, pp. 106–119, 2006.
12. Fraunhofer-Allianz-Vision, "Leitfaden zur hyperspektralen bildverarbeitung," 2019.
13. N. Otsu, "A threshold selection method from gray-level histograms," *IEEE Transactions on Systems, Man, and Cybernetics*, vol. 9, no. 1, pp. 62–66, 1979.
14. J. Yousefi, "Image binarization using otsu thresholding algorithm," *Ontario, Canada: University of Guelph*, 2011.
15. L. Breiman, "Random forests," *Machine learning*, vol. 45, no. 1, pp. 5–32, 2001.
16. L. Bokobza, *Origin of near-infrared absorption bands*. Wiley-VCH, 2002.
17. D. Lestari, A. Rohman, S. Syofyan, N. D. Yuliana, N. K. B. A. Bakar, and D. Hamidi, "Analysis of beef meatballs with rat meat adulteration using fourier transform infrared (ftir) spectroscopy in combination with chemometrics," *International Journal of Food Properties*, vol. 25, no. 1, pp. 1446–1457, 2022.